2

TIP3P and TIP4P/2005 water models for hydration dynamics near membranes

2.1 INTRODUCTION

Water molecules play a crucial role in carrying out various biological functions of the cells as well as DNA, RNA, proteins, lipids by forming an extended hydrogen bond network structure [Bagchi, 2013; Hummer and Tokmakoff, 2014; Jungwirth, 2015; Srivastava and Debnath, 2018]. Various computational and experimental studies report water assisting in functioning of bio-molecules [Pasenkiewicz-Gierula *et al.*, 1999; Smondyrev and Voth, 2002a; Gurtovenko and Vattulainen, 2005; Swenson *et al.*, 2008; Ohto *et al.*, 2015]. Previous studies reveal that water models used in conjunction with one biomolecular system may not be suited for the other. Thus, developing transferable water models for chemically reactive systems and re-parameterizing the water models for predicting biomolecular mechanisms have been topics of an active research over the past few decades [Pestana *et al.*, 2018; Onufriev and Izadi, 2018].

In the last two decades, several water models such as TIPS, SPC, TIP3P, TIP4P/2005, etc. are developed to study characteristic properties of liquid bulk water [Jorgensen, 1981; Berendsen *et al.*, 1981; Jorgensen *et al.*, 1983]. A critical component in development of these water models is the intermolecular potential function for the water dimer. The potential functions are derived from *ab-initio* quantum chemical calculations that can predict all known properties of liquid water. The advantage of using quantum chemical approach is that many of the systems can be treated for which experimentally no data is available. However, the accuracy of these potential functions depends on the basis set used in ab-initio calculations [Jorgensen, 1979].

Simple Point Charge (SPC) water model was initially developed for studying protein hydration [Berendsen *et al.*, 1981]. However, because of its simplicity and capability of reproducing many liquid water properties, it is used for a wide variety of protein and membrane simulations [Tarek and Tobias, 2000; Patra *et al.*, 2003; Jiang *et al.*, 2004; Hu and Jiang, 2010; Hartkamp *et al.*, 2018; Ferrario and Pleiss, 2019]. Structural and dynamical properties such as radial distribution function (RDF) and velocity auto correlation function (VACF) match well with X-ray diffraction data [Narten and Levy, 1971]. Diffusion coefficient for the centre of mass of SPC water is higher than that from NMR data [Mills, 1973].

TIP3P water (Transferable Intermolecular Potential for 3 Point charge) reproduces similar properties of liquid water as the SPC model. The potential functions of TIP3P model are transferable i.e one set of potential function for atoms can be used to construct potential functions for different systems [Jorgensen, 1981]. It is widely used for simulating biological systems due to robustness and compatibility with lipid force fields [Golosov and Karplus, 2007; Tolonen *et al.*, 2015; Ollila *et al.*, 2018]. The first hydration shell of radial distribution function (RDF) of TIP3P water model agrees well with the experimental data, however it is less structured beyond the first hydration shell [Jorgensen *et al.*, 1983]. It also over-estimates the diffusion coefficient of liquid water probably due to weak hydrogen bonding among water molecules [Vega *et al.*, 2009]. A threshold in terms of accuracy has been achieved for three point charge models for molecular simulations of bio-molecules [Izadi and Onufriev, 2016].

TIP4P reproduce liquid water properties better than three point charge models. TIP4P water model has 3 fixed point charges and the lone pair of electrons on the oxygen atom is placed on a dummy atom located at the bisector of H-O-H angle. TIP4P water model is re-parameterized

Table 2.1: Parameters for SPC, TIP3P and TIP4P/2005 water models.

Parameters	SPC [Berendsen *et al.*, 1981] [Jorgensen *et al.*, 1983]	TIP3P [Jorgensen *et al.*, 1983]	TIP4P/2005 [Abascal and Vega, 2005] [Benavides *et al.*, 2017]
$\angle$ HOH (in ^{o})	109.28	104.52	104.52
δ^- (O)	0.82	0.84	0
δ^+ (H)	0.410	0.417	0.554
δ^- (dummy)	-	-	-1.1128
r_{OH} (in Å)	1.00	0.9572	0.9572
σ (in Å)	3.166	3.1506	3.1589
ϵ_{OO} (in kcal/mol)	1.31	1.19	0.1852

to TIP4P/2005 water model which incorporates properties of ice and density maximum of the 3-site model, giving accurate results over a wide range of properties [MacDowell and Vega, 2010; González and Abascal, 2010; Sedlmeier *et al.*, 2011; Guevara-Carrion *et al.*, 2011; Stirnemann and Laage, 2012].

The water models are developed based on the parameters such as number of charges, H-O-H angle, bond distance between O-H, non-bonded interaction parameters, etc. The parameters for SPC, TIP3P and TIP4P/2005 are mentioned in table 2.1.

Force fields (FF) are generally described by mathematical expressions which describe energy dependency of the system on particle coordinates. Force fields contain interatomic potential energies in analytical form and some set of parameters. The set of parameters are obtained from *ab-initio* quantum chemical calculations. The quality of FFs dictate the accuracy of MD simulations. FF for several biomolecules are tested and parameterized for having the best possible representation of biomolecular systems. Since the basis of the FFs are quantum chemical calculations, accuracy of *ab-initio* computations plays a crucial role in determination of intramolecular interactions and atomic charges. For biomolecular simulations, a variety of force fields exist classified in terms of their potential function and parameterization. Over the past few decades, many force fields are developed for biomolecular simulations viz. GROMOS (Groningen Molecular Simulation package) [Berendsen *et al.*, 1984a; Schuler *et al.*, 2001; Chandrasekhar *et al.*, 2003], CHARMM (Chemistry at Harvard Macromoecular Mechanics) [MacKerell *et al.*, 1995, 1998], AMBER (Assisted Model Building and Energy Refinement) [Damodaran *et al.*, 1992; Essmann *et al.*, 1995a], Slipids [Jämbeck and Lyubartsev, 2012a,b] and so on.

GROMOS force field is a united atom force field where each of the non-polar CH_3, CH_2 and CH group is represented as a single bead which allows speeding up of the molecular simulations. Berger force field is derived from GROMOS force field where Lennard-Jones (LJ) parameters for CH_n group are optimized to reproduce condensed phase properties of pentadecane. Adjustment of LJ parameters for CH_n group results in correct reproduction of bilayer properties such as density profile, deuterium order parameter and area per lipid for saturated and unsaturated phospholipids in liquid crystalline phase [Lyubartsev and Rabinovich, 2016] from NMR, neutron scattering and infrared spectroscopic experiments [Poger and Mark, 2010; Poger *et al.*, 2010]. CHARMM force field is an all atom force field which has hydrogens specified explicitly for each non-polar CH_3, CH_2 and CH group. Since CHARMM has full atomistic description, it seems to have advantage in capturing bilayer properties. CHARMM36 force field is derived from CHARMM and is validated over a wide range of lipid bilayers [Jójárt and Martinek, 2007; Rosso and Gould, 2008; Siu *et al.*, 2008].

The surface pressure-area isotherms for DPPC and POPC monolayers are found to be in near quantitative agreement with experiments when OPC4 water model is combined with CHARMM36 lipid force-field [Javanainen *et al.*, 2018]. A fully hydrated 1,2-dispalmitoyl-sn phosphatidylcholine (DPPC) bilayer is simulated in presence of TIP4P/2005 water model for evaluating optimal

temperature which fulfills equipartition theorem and agrees well with the experiments [Jung *et al.*, 2019]. Several experimental investigations on dynamics of water have been reported revealing confinement and slowing down of water relaxation near bio molecules. The time scale for lateral diffusion of water molecules near lipid bilayers is of the order of several nanoseconds which is characterized by a further decrease in diffusion coefficient [von Hansen *et al.*, 2013]. Neutron scattering experiments and dynamic structure factor along with molecular dynamics simulation of TIP3P water model provide a microscopic mechanism of water structural relaxation [Arbe *et al.*, 2016]. However, till date, a general consensus has not been established regarding the water model which can capture the structure and dynamics of water in presence of lipid bilayers as quantitatively as in bulk water keeping the lipid properties in accordance with experimental investigations. It is therefore a formidable task to wisely select a water model that can capture various properties of fully hydrated lipid bilayers.

Thus, in the current chapter, we attempt to compare the structure and dynamics of hydration layers of a DMPC lipid bilayer using Berger and CHARMM36 force fields in combination with TIP3P and TIP4P/2005 water models at 308 K. Although comparative studies of bulk water models have been reported previously [Jorgensen *et al.*, 1983; Vega *et al.*, 2009] none of the studies confirm if the same comparisons will be valid for hydration layers of lipid bilayers. Pair correlation functions of oxygen atoms in hydration layers of lipid bilayers are calculated. The study envisages the effect of chemical confinement of the hydration water on its local structure. For characterizing dynamical behavior manifested by both water models in presence of DMPC, anomalous diffusion exponents are calculated for water molecules in the hydration layer. Non-Gaussian parameters (NGP), velocity auto-correlation functions (VACF) and displacement maps are calculated for both models to investigate the glassy dynamics invoked in interface water molecules in presence of DMPC head groups. The analysis a) tests the suitability of TIP3P and TIP4P/2005 water model in presence of Berger and CHARMM36 force-fields for investigating structure and dynamics of water near lipid bilayers, b) confirms the existence of fluid phase of the DMPC bilayer at 308 K as in experiments when the water models are used in combination with the lipid force fields, c) provides the microscopic structure of the interfacial water molecules near the bilayer, d) indicates the presence of dynamical heterogeneities in interfacial water at temperature well above supercooling.

2.2 SIMULATION DETAILS

All atom molecular dynamics simulations are carried out for 128 DMPC lipid molecules solvated with a) TIP3P [Mark and Nilsson, 2001] and b) TIP4P/2005 [Abascal and Vega, 2005] water models with 6005 and 5743 water molecules respectively where the bilayers are in fully hydrated state [Lopez *et al.*, 2004; Zhao *et al.*, 2008; Trapp *et al.*, 2010]. Figure 2.1 a) and 2.1 b) show single DMPC molecule and the bilayer demonstrating interface water. Table 2.2 shows the detail of the systems studied based on the type of water models used. For DMPC lipids using Berger force field [Berger *et al.*, 1997; Cordomí *et al.*, 2012] two NPT simulations are carried out for 300 ns and 100 ns with 2 fs time steps for a) TIP3P and b) TIP4P/2005 respectively. A DMPC bilayer using CHARMM36 force field [Klauda *et al.*, 2010; Zhuang *et al.*, 2014; Khakbaz and Klauda, 2018] (system c in table 2.2) is simulated for 500 ns with a 2 fs time step for TIP4P/2005 water model. CHARMM36 in combination of TIP3P is not used since TIP4P/2005 of system b) (table 2.2) performed better than system a) (table 2.2) in capturing the hydration dynamics. All the three systems (table 2.2 a), b) and c)) are equilibrated at 308 K temperature using velocity rescaling method [Bussi *et al.*, 2007] with a coupling constant of 0.50 ps. Pressure is maintained at 1 bar using Berendsen pressure coupling [Berendsen *et al.*, 1984b] method for all systems. Both van der Waals and Coulombic interactions are cutoff at 1 nm and long range interactions are corrected using Particle Mesh Ewald (PME) method with a grid size of 0.12 nm. Next, for systems a), b) and c), NVT runs are carried out for 5 ns, 1 ns and 2 ns respectively with a time step of 0.4 fs. All bonds are constrained using the LINCS [Hess *et al.*, 1997] algorithm during equilibration. Next 100 ps NVT runs are carried out with a time step of 0.4 fs without constraints for all systems. Area per

Table 2.2: Categorization of hydrated systems based on force fields and water models.

	System	Water Model	Simulation box size (in nm)
a)	Hydrated DMPC (Berger)	TIP3P	$6.30 \times 6.30 \times 8.01$
b)	Hydrated DMPC (Berger)	TIP4P/2005	$6.24 \times 6.24 \times 7.95$
c)	Hydrated DMPC (CHARMM36)	TIP4P/2005	$6.27 \times 6.27 \times 7.91$
d)	Bulk Water	TIP3P	$3.75 \times 3.75 \times 1.87$
e)	Bulk Water	TIP4P/2005	$3.69 \times 3.69 \times 1.84$

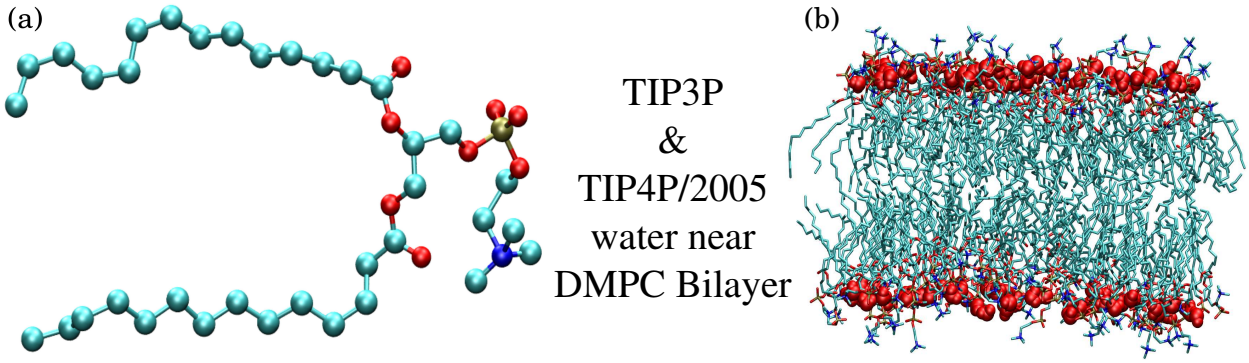

Figure 2.1: Snapshot of a) single DMPC molecule and b) DMPC bilayer in presence of interfacial water shown in red. All water molecules are not shown for clarity.

head group of the lipids and other properties such as temperature, pressure of the systems from the production runs in absence of constraints match well with that of the equilibration runs confirming the stability of the simulations without contraints. For the calculation of lipid diffusivities, 100 ns NVT runs are carried out for system a)-c) in table 2.2 with the same set of parameters as mentioned before. Periodic boundary conditions are applied in all the three directions. Trajectories are saved at every 10 fs.

For comparing dynamics of water present in hydration layers of DMPC with the properties of bulk water, only bulk water molecules (BW) are simulated without DMPC lipids consisting of 851 water molecules of both models (table 2.2 d) and e)). NPT runs are carried out for 2 ns followed by 100 ps NVT runs where all bonds are constrained with LINCS. Next, 100 ps NVT runs are carried out with a time step of 0.4 fs and a saving frequency of 10 fs without constraints for both the models for the production runs. All other parameters are kept same as in the hydrated DMPC systems. For the calculation of velocity auto correlation function (VACF), an extra NVT simulation for 10 ps is run with a 0.4 fs time step and a 0.4 fs saving frequency for all five systems. All simulations are carried out using GROMACS-4.6.5 software package [Bekker *et al.*, 1993; Berendsen *et al.*, 1995; Lindahl *et al.*, 2001; Spoel *et al.*, 2005; Hess *et al.*, 2008; D. van der Spoel and the GROMACS development team., 2013]. $10,000$ time origins of the last 100 ps production runs are used for calculating dynamical properties. No constraints are applied on the production run.

2.3 LIPID BILAYER PROPERTIES

All systems mentioned in table 2.2 are simulated at physiological temperature, 308 K, at which the bilayer exists in liquid crystalline (L_α) phase [Purusottam *et al.*, 2015]. For gaining

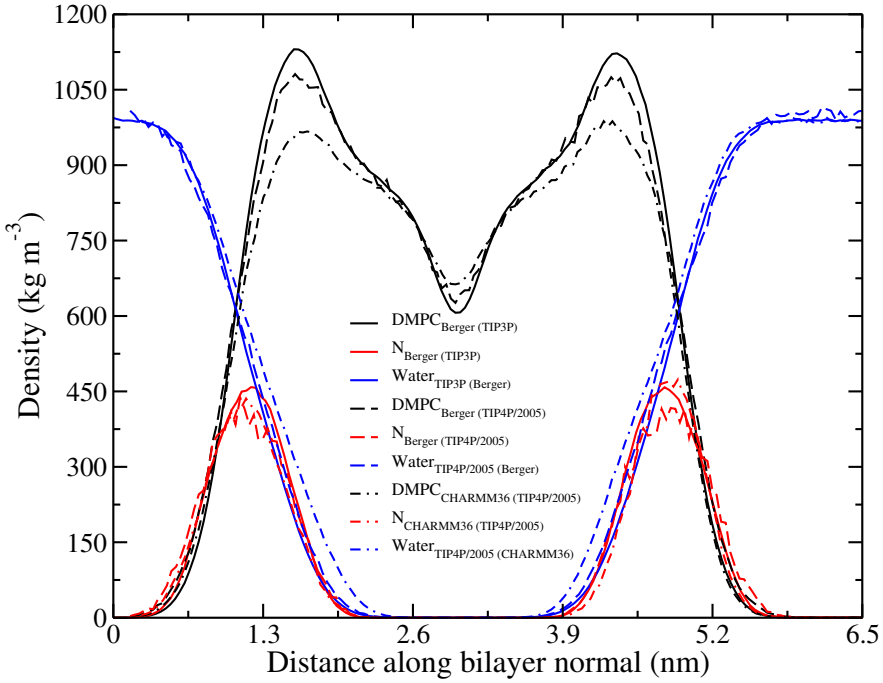

Figure 2.2: Density profile of DMPC bilayer from Berger and CHARMM36 force fields hydrated with TIP3P and TIP4P/2005 water. Solid lines : Berger bilayer with TIP3P water model, Dashed lines: Berger bilayer with TIP4P/2005 water model and Dashed dot lines show CHARMM36 bilayer with TIP4P/2005 water model. For clarity, density distribution of Nitrogen (N) is multiplied by a factor of 10.

deeper insights on the structure of the examined systems, average density profiles are calculated for individual components of the hydrated DMPC system. Figure 2.2 show density distributions of DMPC and water along the bilayer normal for systems a), b) and c) mentioned in table 2.2 using both water models. The density distributions show the location of DMPC, nitrogen head-group and water along the bilayer normal (z-axis). The two peaks for nitrogen atoms and DMPC molecules correspond to the upper and lower leaflets. However, the density profile for DMPC does not decay to zero near mid-plane ($\sim$ 3.4 nm along bilayer normal, figure 2.2) due to presence of the acyl chains. Density profiles for both water models in combination with Berger and CHARMM36 force fields agree well with each other.

Bilayer properties are quantified by measuring following parameters viz. area per head-group (a_h), bilayer thickness (d), deuterium order parameter (S_{CD}), lateral diffusion coefficient (D_L) and surface tension (γ_s). a_h is the time averaged lateral dimensions of the simulation box ($<A_{xy}>$) divided by the number of lipid molecules in each leaflet (n_l) ($<a_h> = <A_{xy}>/n_l$). d is defined as the peak to peak distance between the N head-group density of the lipids of two leaflets (figure 2.2). A representation of d is shown in figure 2.3. Ordering of acyl chains of the bilayer is calculated by S_{CD}. It describes the angle of C-D bond vector with respect to the bilayer normal. Experimentally order parameter are measured by ^{2}H NMR spectroscopy techniques [Nagle and Tristram-Nagle, 2000]. In simulations, for all atom force fields, S_{CD} is given as $S_{CD} =< 3cos^2\theta - 1 > /2$ [Seelig and Niederberger, 1974; Stockton *et al.*, 1976], where θ is the angle of C-D bond vector with respect to the bilayer normal. However, for united atom force fields, obtaining S_{CD} is not straight forward as hydrogen atoms are not explicitly specified. Let us suppose that atom C_n is the atom of interest for S_{CD} calculation. Then Z-axis is chosen as the vector from C_{n+1} to C_{n-1} bead of the lipid (shown by yellow color beads of figure 2.4 a)). A plane containing C_n bead and C_n-H atom is constructed (shown by grey color triangle in figure 2.4 a)). The positions of H atoms are predicted based on the structure of the methylene group. X-axis is defined perpendicular to z-axis and Y-axis

is perpendicular to both X and Z axes (figure 2.4 a)) [van der Ploeg and Berendsen, 1982]. Then, the order parameter is given as, $S_{CD} = \frac{2}{3}S_{xx} + \frac{1}{3}S_{yy}$, where S_{xx} and S_{yy} are order parameter along x and y axis respectively [Piggot *et al.*, 2017]. Translational mean square displacement in three-dimensional space is calculated using equation 2.1.

$$< r^2(t) >= \frac{1}{N}\sum_{i=1}^{N} < [r_i(t+t') - r_i(t')]^2 >_{t'} \tag{2.1}$$

where, $r = \sqrt{x^2+y^2+z^2}$, denotes distance in three dimensional space, t' is the time origin, t is the difference and summation runs over total number of water molecules. The angular bracket denotes the average over time origins. For two dimensional systems, r becomes, $r = \sqrt{x^2+y^2}$. Thus, the lateral diffusion constant, D_L, becomes,

$$D_L = \lim_{t\to\infty} \frac{1}{4}\frac{d}{dt} < [\Delta r_i(t)^2] > \tag{2.2}$$

γ_s is defined as the surface property of a liquid allowing it to resist an external force. The resistance exhibited by the liquid surface is due to cohesive nature of its molecules. γ_s for lipid bilayer under ideal conditions, where there are no concentration gradients across the membranes, should be 0 as free energy should be minimum with respect to the membrane surface area [Jähnig, 1996; Brochard-Wyart *et al.*, 1976]. γ_s is obtained by calculating the pressure tensor components viz. P_{xx}, P_{yy}, P_{zz} [Rose *et al.*, 2008] and substituting them in the following equation,

$$\gamma_s = h_z\big(P_{zz} - \big(\frac{P_{xx}+P_{yy}}{2}\big)\big) \tag{2.3}$$

where, P_{xx}, P_{yy} and P_{zz} are pressure tensor components along x, y and z direction respectively and h_z is the z-component of the box dimension. a_h, S_{CD} and d of the bilayer using Berger force fields are consistent with that obtained from experiments (table 2.3) at the fluid phase. CHARMM36 force field in presence of TIP4P/2005 is found to slightly overestimate the a_h , S_{CD} and d compared to the experimental data at fluid phase (table 2.3). Order parameter for all the three systems a), b) and c) mentioned in table 2.2 are consistent with that of the experiments of lipid bilayer at the fluid phase. D_L for DMPC of system a), b) and c) mentioned in table 2.3 are calculated once they reach diffusive regime (table 2.3). Berger lipids in combination with TIP3P water model over-estimates the diffusivities compared to the experiments. The diffusion constants of bilayers with Berger and CHARMM36 force-fields in combination with TIP4P/2005 water model match well with the experimental values [Almeida and Vaz, 1995]. However, the lipid diffusivities for all three cases have similar ranges as the previous performed simulations of CHARMM27 lipids in combinations with TIP3 water model or Berger lipids in combination with SPC water model [Högberg and Lyubartsev, 2006; Flenner *et al.*, 2009]. Berger lipids in combination with TIP3P water model over-estimates the surface tension compared with the reported literature. The surface tension of the lipid bilayer-water interface with Berger and CHARMM36 force-fields in combination with TIP4P/2005 water model match well with the reported literature values [Tieleman and Berendsen, 1996; Chiu *et al.*, 1995]. The overall analyses dictate the suitability of Berger force field in conjunction with both water models to identify the interface of the equilibrated DMPC bilayer at fluid phase.

2.4 CLASSIFICATION OF WATER REGIMES

To decouple the contribution of bulk water (BW) molecules to the dynamical properties of hydration layers, we identify water molecules continuously residing in the first hydration shell of the N head-groups as interfacial water (IW). The first hydration shell of DMPC head-group (nitrogen-atom) is identified by calculating radial distribution function (RDF) between O_{water}-N_{Lipid} using the following equation,

$$g(r) = \left\langle \frac{1}{\rho_N}\sum_{i=1}^{N}\sum_{i=1}^{N}\delta(r_{ij}-r)\right\rangle \tag{2.4}$$

Table 2.3: Area per head-group (a_h), bilayer thickness (d), deuterium order parameter ($|S_{CD}|$), lateral diffusivity (D_L) and surface tension (γ_s) of the DMPC bilayer from our simulations and previously performed experiments at 308 K.

		TIP3P (Berger)	TIP4P/2005 (Berger)	TIP4P/2005 CHARMM36
a_h (nm^2)	Simulation	0.59 ± 0.01	0.61 ± 0.03	0.62 ± 0.01
	Experiment	0.60 [Kučerka *et al.*, 2011]		
d (nm)	Simulation	3.65 ± 0.21	3.54 ± 0.22	3.67 ± 0.21
	Experiment	3.60 [Nagle and Tristram-Nagle, 2000]		
$-S_{CD}$	Simulation	0.17 ± 0.03	0.15 ± 0.03	0.195 ± 0.03
	Experiment	~ 0.18 [Petrache *et al.*, 2000] [Aussenac *et al.*, 2003]		
D_L ($\times 10^{-7} cm^2 s^{-1}$)	Simulation	1.80 ± 0.016	0.33 ± 0.01	0.82 ± 0.002
	Experiment	0.69 [Almeida and Vaz, 1995] [Flenner *et al.*, 2009]		
γ_s (mN cm^{-1})	Simulation	31.46	26.61	29.56
	Simulation (Literature)	28.00 [Tieleman and Berendsen, 1996] [Chiu *et al.*, 1995]		

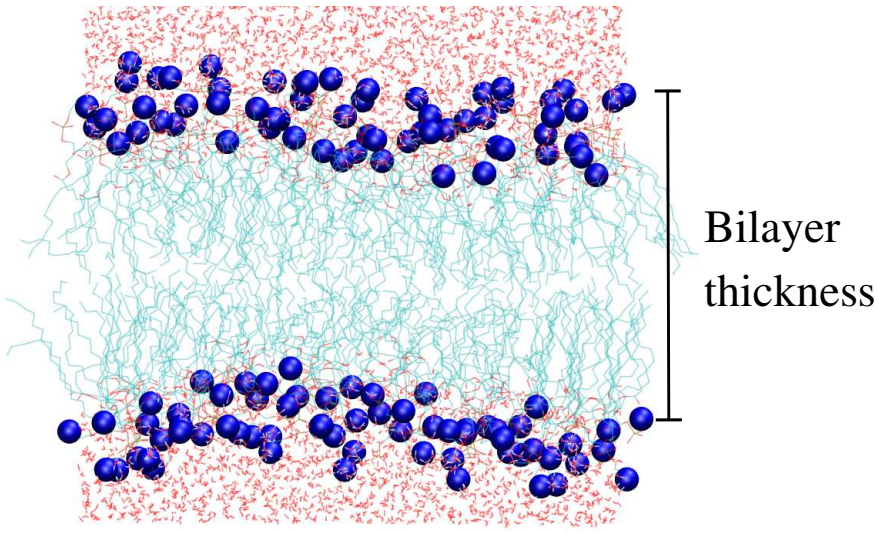

Figure 2.3: Snapshot showing the bilayer thickness (d) using VMD [Humphrey *et al.*, 1996]. Color code: blue nitrogen atoms of DMPC head-groups.

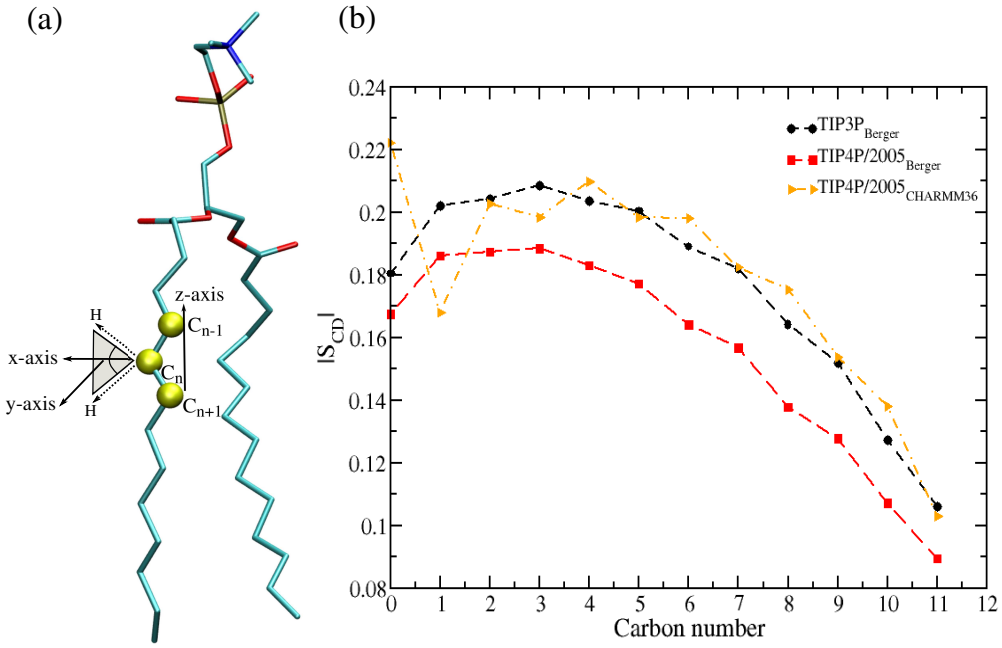

Figure 2.4: a) Snapshot of single DMPC molecule showing acyl chain beads for order deuterium order parameter calculation. Color code: green vdw methylene beads of acyl chains. H predicted hydrogen atoms for united atom force fields associated with the methylene group. b) Deuterium order parameter of the DMPC bilayer hydrated with TIP3P and TIP4P/2005 water models are reasonably consistent with each other.

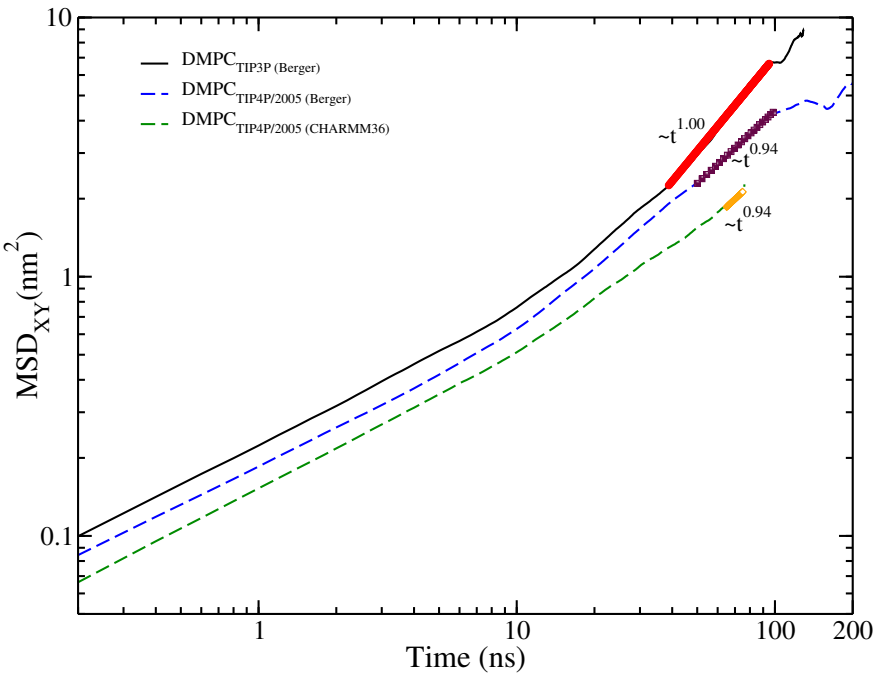

Figure 2.5: Lateral mean square displacements of the DMPC bilayer hydrated with TIP3P and TIP4P/2005 water models. All three systems a), b) and c) mentioned in table 2.2 reach diffusive regimes within 100 ns.

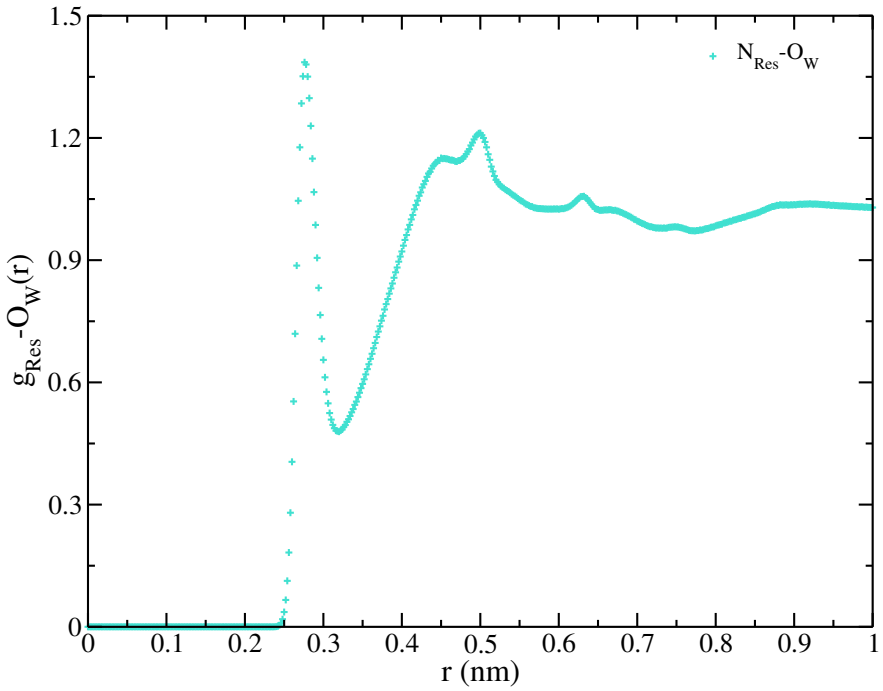

Figure 2.6: Pair correlation function between nitrogen (N) atom of DMPC head and oxygen atom of water.

where, ρ_N is number density and angular bracket show ensemble averaging. The first hydration shell of nitrogen head-group corresponds to the first peak of the RDF ($\sim$ 0.3 nm in figure 2.6). For probing residence time of IW, survival probability (S(t)) is calculated. S(t) is the probability of finding water molecule residing in a given layer d at time t. Mathematically, it is given as,

$$S(t) = \sum_{i=1}^{N} \langle \prod_{t_k=t_0}^{t_0+t} P_i^d(t_k) \rangle \tag{2.5}$$

where, $P_i^d(t)$ is defined as the probability associated with i$^{\text{th}}$ molecule to reside in a given layer d at time t. $P_i^d(t) = 1$ if the molecule is present in layer d at time t and $P_i^d(t) = 0$ otherwise. Angular bracket denotes averaging over time origins and summation runs over the total number of molecules. Figure 2.7 show the survival probability of IW calculated for 1 ns time window with 1 ps sampling frequency. The residence time for interface water is obtained by fitting the plot (figure 2.7) with a bi-exponent function ($y = A_f exp\left(-\frac{t}{\tau_f}\right) + A_s exp\left(-\frac{t}{\tau_s}\right)$) and the characteristic residence time scales are mentioned in table 2.4. Interfacial water show two characteristic residence time scales viz. fast (τ_f) and slow (τs) as mentioned in table 2.4. For capturing IW water dynamics, the residence time should be long enough for obtaining a reasonable statistics. Thus, 100 ps corresponding to slow residence time (τ_s) from table 2.4 is chosen as the confinement lifetime or residence lifetime for all calculations.

Although the definition of IW include most of the water molecules which may be hydrogen bonded to oxygen atoms present in different chemical moieties of DMPC head-groups [Debnath *et al.*, 2010], it does not guarantee to include the complete set of IW which are hydrogen bonded to the carbonyl oxygens buried deepest in the hydrophobic region of the membrane. There are 21 TIP3P and 104 TIP4P/2005 IW for the DMPC bilayer with the Berger force field and 84 TIP4P/2005 IW for the DMPC bilayer with the CHARMM36 force field when 100 ps time window is considered as the confinement lifetime. Since TIP3P water is known to be more diffusive than TIP4P/2005 [Krynicki *et al.*, 1978a; Vega *et al.*, 2009] less number of IW molecules are found for continuously residing TIP3P IW compared to TIP4P/2005 IW molecules. Figure 2.1 b) shows a snapshot of IW

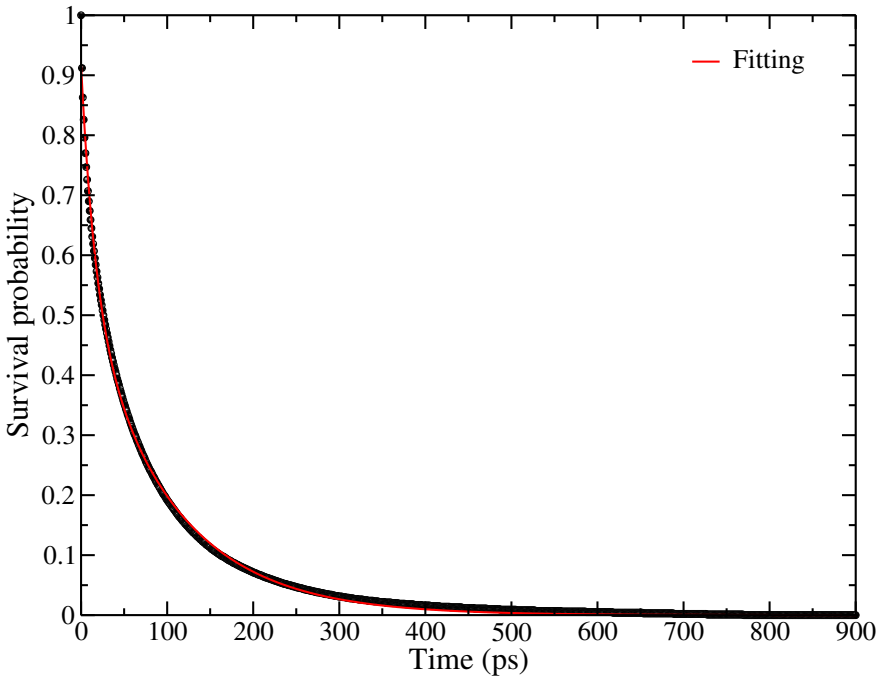

Figure 2.7: Survival probability of water residing at DMPC head-group surface.

Table 2.4: Residence time scales for water computed over 1 ns time window with sampling frequency of 1 ps. Correlation coefficient is >0.99

A_f	τ_f (ps)	A_s	τ_s (ps)
0.38	16.40	0.54	99.56

in presence of DMPC lipid bilayer for a single time frame. For predicting the applicability of the water model, several structural and dynamical properties of IW corresponding to three systems are investigated. For validating these findings, structure and dynamics of all IW are compared with BW.

2.5 PAIR CORRELATION FUNCTIONS

The spatial two-body correlations between water molecules are studied due to the possibility of direct comparison with neutron scattering and X-ray diffraction experiments [Skinner *et al.*, 2016]. The RDF (g(r)) between oxygen and oxygen (figure 2.8 a)) and oxygen and hydrogen atoms of water molecules (figure 2.8 b)) are calculated for all five systems mentioned in table 2.2 using equation 2.4. The intra-molecular interactions are omitted. The RDFs for the bulk water molecules (BW) from both the models agree well with each other and agree with the previously performed experiments as well [Skinner *et al.*, 2013, 2016]. The width of the first peak in figure 2.8 (a) slightly increases from the BW to the IW followed by an emergence of a shoulder for the IW. In order to quantify the effect of hydrogen bonding on water arrangements, oxygen-hydrogen RDF is calculated (figure 2.8 b)). The O-H RDFs of the IW molecules for all systems show enhancements in amplitudes of the first and second peaks compared to that of the BW. This is due to hydrogen bond network for chemically confined IW where one IW can be hydrogen bonded to another IW and concertedly

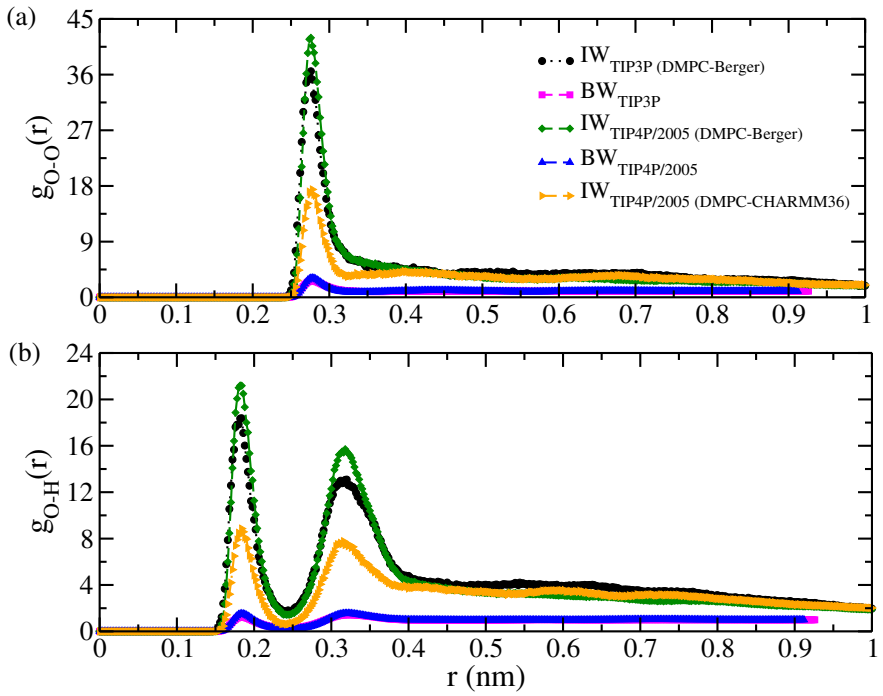

Figure 2.8: Pair correlation functions between a) oxygen-oxygen of IW and BW, b) oxygen-hydrogen of IW and BW.

hydrogen bonded to lipid head moieties [Srivastava and Debnath, 2018]. Since the volume of all water are normalized, the higher amplitudes of IW compared to the BW are due to the more available donor sites of water molecules to the oxygen atoms of DMPC heads. This indicates an increase in coordination numbers in the IW of both the water models in presence of the lipid bilayer.

2.6 ANOMALOUS DIFFUSION EXPONENT

Since lipid bilayers are asymmetric along the bilayer surface (xy) and the normal (z), dynamical properties of water near the bilayer is investigated by calculating lateral translational mean square displacement (MSD) of H atom using equation 2.1. Then diffusion exponent is calculated by logarithmic differentiation of translational MSD as [Wassenaar *et al.*, 2013],

$$\alpha(t) = \frac{\partial ln(< r^2(t) >)}{\partial t} \tag{2.6}$$

where α(t) denotes the type of diffusion. For short time scales (sub-picosecond), $\alpha \sim 2$ denotes a ballistic regime, $\alpha < 1$ denotes a sub-diffusive regime and $\alpha \sim 1$ denotes a diffusive regime. Fig. 2.9 shows that the BW from both models exhibit an α close to 1 depicting diffusive regime, whereas the IW from both models show $\alpha < 1$ denoting sub-diffusive behavior due to confined nature near lipid heads. Similar sub-diffusivity is reported earlier for water molecules near MGDG and DOPC bilayers [Markiewicz *et al.*, 2015]. Since BW reach the diffusive limits for both models, translational self diffusion coefficient is calculated only for the BW using the following equation in 3 dimensions,

$$D_{trans} = \lim_{t\to\infty} \frac{1}{6}\frac{d}{dt} < [\Delta r_i(t)^2] > \tag{2.7}$$

Table 2.5 represents self diffusion coefficient of BW using both models. Self diffusion coefficient (D) of TIP4P/2005 water from our calculations agrees well with the previously reported literature at

Table 2.5: Diffusion constants (D_{trans}) (in 10^9 D, m^2s^{-1}) calculated from VACF and MSD of BW for both models.

	Water Model	from MSD	from VACF
Simulations	TIP3P	7.00 ± 0.29	6.84
	TIP4P/2005 (308 K)	2.46 ± 0.25	2.65
	TIP4P/2005 (298 K)	2.03 ± 0.34	
Experiments		2.89 (at 308 K)[Holz *et al.*, 2000] [Mills, 1973]	
		2.33 (at 298 K)[Krynicki *et al.*, 1978b]	

298 K and 308 K [Krynicki *et al.*, 1978a; Vega *et al.*, 2009]. However, TIP3P BW is known to have higher D_{trans} due to the presence of weak hydrogen bonding in TIP3P water model [Vega *et al.*, 2009].

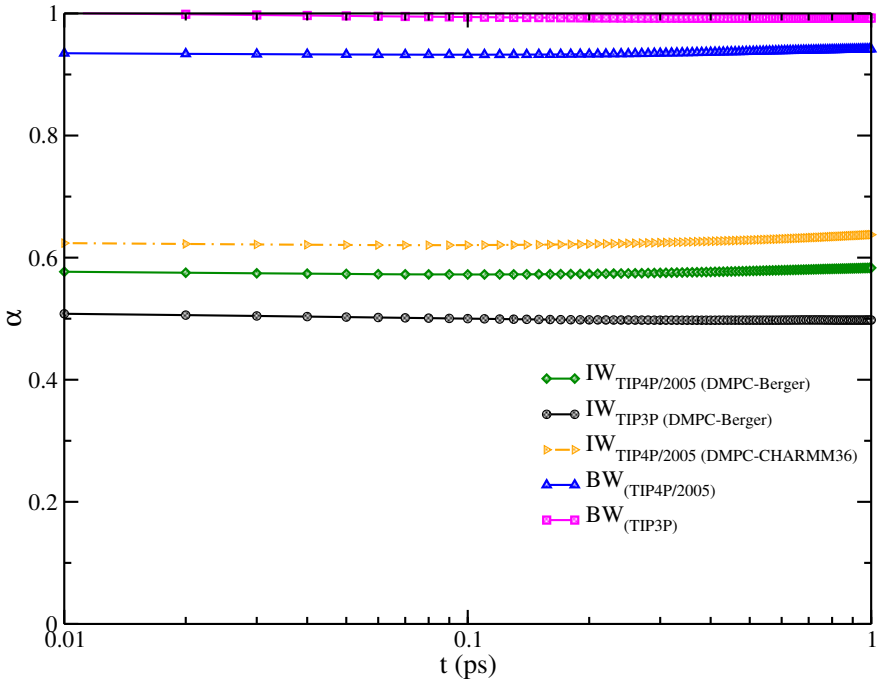

Figure 2.9: Anomalous diffusion exponent (α) as a function of time showing the type of diffusion for the IW and the BW for both water models. Fluctuations at longer times are not shown. Both TIP3P and TIP4P/2005 bulk water are diffusive where the IW are sub-diffusive in nature.

2.7 VELOCITY AUTO CORRELATION FUNCTION

Velocity auto correlation function (VACF) is a dynamical quantity characterizing the stochasticity proliferated in a molecular system. Amplitudes of VACF corresponds to the inter-particle collisions in the system. To study such stochasticity in the interface water, translational VACF for the IW and the BW are calculated using following equation,

$$C_V(t) = \frac{1}{N}\sum_{i=1}^{N}\frac{< v_i(t_0).v_i(t) >}{< v_i(t_0).v_i(t_0) >} \tag{2.8}$$

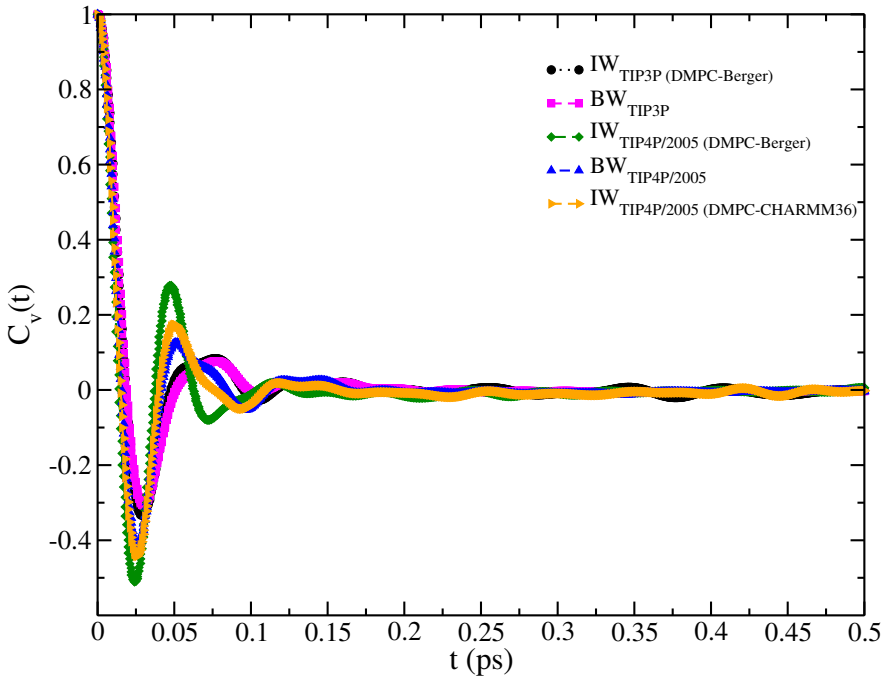

Figure 2.10: VACF of IW and BW using TIP3P and TIP4P/2005 water models (for IW in presence of Berger and CHARMM36 lipids). IW show deeper minima than the BW suggesting more back-scattering from the oscillations of IW cages formed by the neighboring molecules via hydrogen bonds.

where N denotes total number of particles, $v_i(t_0)$ represents velocity at initial time and $v_i(t)$ shows velocity at time t. There are well defined negative minima in VACF of all cases indicating velocity reversal of particles due to inter-molecular collisions (figure 2.10). Among all five sets, the minimum in VACF lies for $IW_{TIP4P/2005\ (DMPC\text{-}Berger)}$ in comparison with the rest of the cases and the long range correlation persists more for IW compared to the BW. The confined IW exhibit a rattling motion inside a cage governed by the hydrogen bonded network to the oxygen atoms of the lipid head groups. This indicates a possibility of glassy dynamics to the IW using both models. BW, on the other hand, have no influence from the lipid head-groups, thereby possessing shallower negative minima in comparison with the IW. It is widely believed that as compared to translational MSD, VACF converges faster [Allen and Tildesley, 1987], therefore we computed self diffusion coefficient of BW using both VACF and translational MSD approach. Self diffusion coefficient computed using VACF is given by Green-Kubo relation,

$$D_A = \frac{1}{3}\int_0^\infty < v_i(t).v_i(0) >_{i\in A} dt \tag{2.9}$$

A comparison between diffusion coefficient of BW obtained from VACF and MSD is made in table 2.5. The values of diffusion constants from VACF and MSD for BW of the same model agree well with each other.

2.8 NON GAUSSIAN PARAMETER

Since translational dynamics and VACF indicate the possibility of presence of glassy dynamics in IW in all combinations of force-fields, the glassy behavior is examined by calculating non-Gaussian parameter (NGP) for hydrated DMPC systems and contrasted with the BW systems.

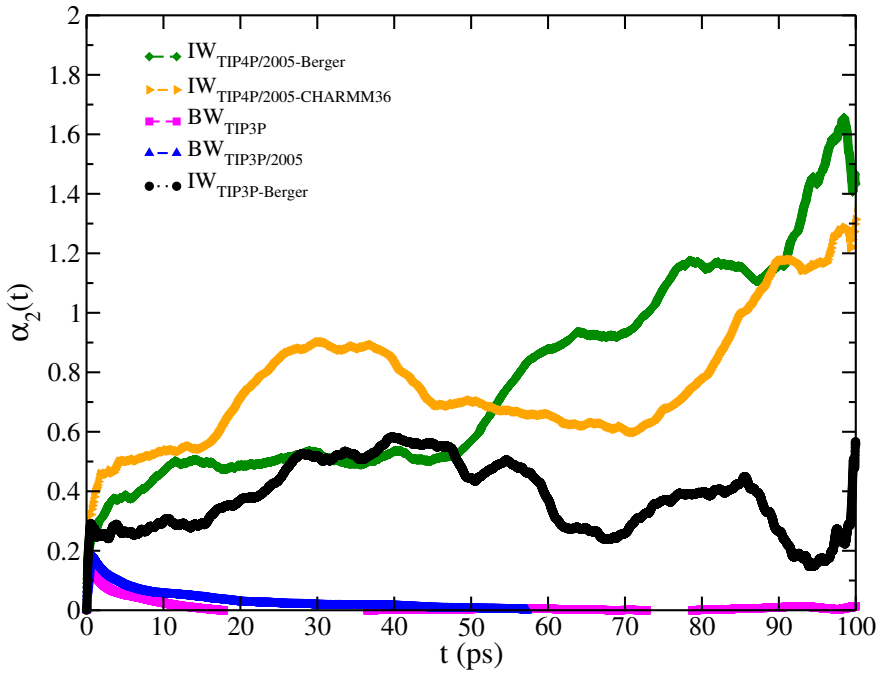

Figure 2.11: NGP of IW and BW for both water models. NGP of BW of both models increase within a very short time and then asymptotically decay to zero showing underlying Fickian dynamics. NGP of IW show non-zero α_2(t) for all combinations of force-fields indicating the presence of dynamical heterogeneity.

For materials showing dynamical heterogeneity, NGP is given by [Rahman, 1964],

$$\alpha_2(t) = \frac{< \Delta r(t)^4 >}{(1 + 2/d) < \Delta r(t)^2 >^2} - 1 \tag{2.10}$$

For a truly Gaussian system, α_2(t) = 0. Here, $\delta r(t) = r(t_0 + t) - r(t_0)$ is particle displacement after a time interval t, d is the spatial dimension and angular bracket represents ensemble averaging. For TIP3P BW, NGP increases for initial 0.68 ps indicating cage-like behavior. At the onset of 0.70 ps, the NGP starts decaying asymptotically to zero. This relaxation time scale from our calculation is consistent with previously reported time scale for TIP3P water model and neutron scattering experiments [Arbe *et al.*, 2016]. BW start diffusing thereby escaping the cage and gradually entering in the diffusive regime following Gaussian dynamics. Very similar behavior is observed for the BW TIP4P/2005 (figure 2.11). For $IW_{TIP3P\text{-}Berger}$, NGP increases till 44.85 ps indicating trapping of water molecules due to strong hydrogen bonded network in the vicinity of lipid head-groups. Afterwards, NGP gradually decreases allowing the molecules to slowly leave the caged environment. $IW_{TIP4P/2005\ (DMPC\text{-}Berger)}$ and $IW_{TIP4P/2005\ (DMPC\text{-}CHARMM36)}$ exhibit an increase in α_2 throughout the confinement time due to the stronger hydrogen bonds of water molecules to lipid head-groups and thus the molecules are trapped for the entire production run. The peaks of α_2(t) are indicative of transition from transient cage to escape from cage generally referred to as β-α relaxation [Stein and Andersen, 2008]. Thus, IW for all combinations prominently show glassy dynamics due to hydrogen bonded network for both TIP3P and TIP4P/2005 water models and BW exhibit Fickian dynamics. Displacement maps of water molecules in all classes are calculated with a time difference obtained from the peak of the NGP to characterize the heterogeneity length scales due to the glassy nature of the interface water.

Figure 2.12 represent the displacement maps for the IW and the BW for both models. The displacements are mapped on the bilayer surface where the length of each arrow represents the magnitude of displacement of individual water molecule in a time-scale when the molecule does a cross-over from the vibration in a cage to diffusion from the cage. Since the number of IW are less

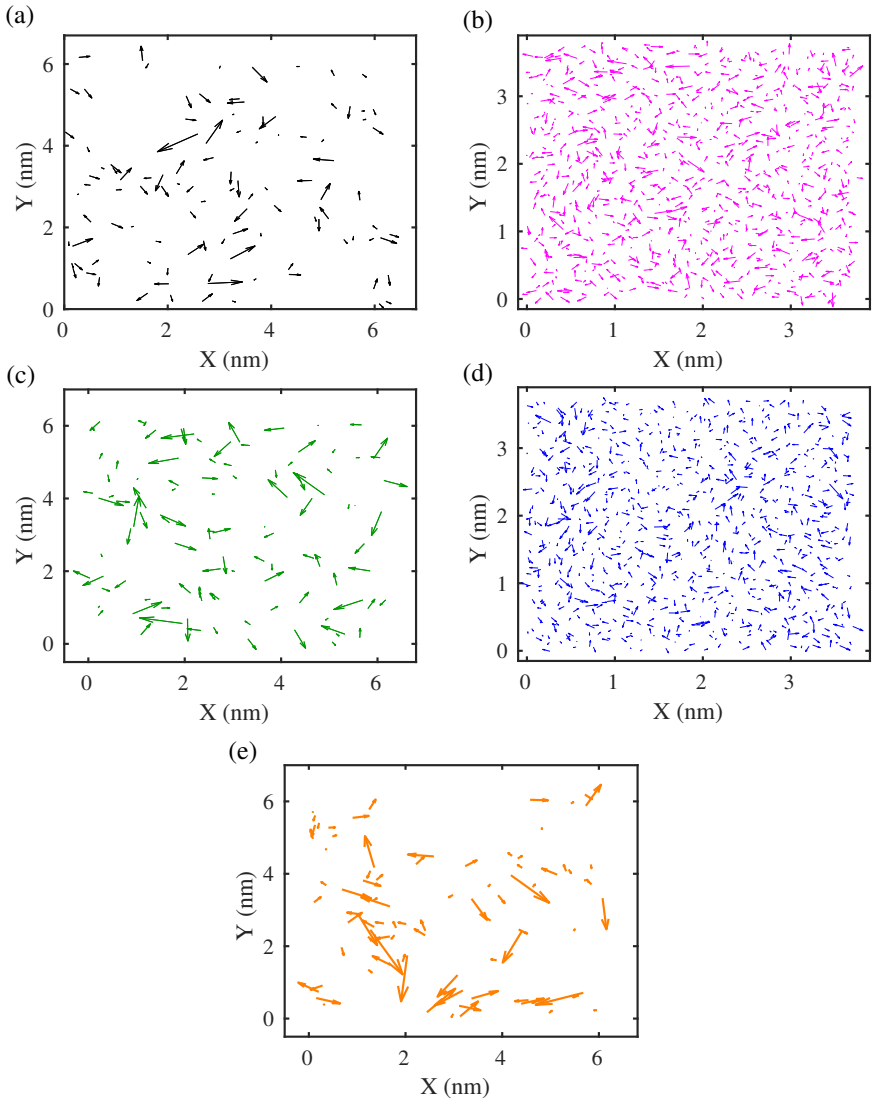

Figure 2.12: Displacement map for a) $IW_{TIP3P\ (DMPC\text{-}Berger)}$, b) BW_{TIP3P}, c) $IW_{TIP4P/2005\ (DMPC\text{-}Berger)}$, d) $BW_{TIP4P/2005}$ and e) $IW_{TIP4P/2005\ (DMPC\text{-}CHARMM36)}$ at respective β-α relaxation time scales. The displacements are mapped on the bilayer surface.

than that of the BW, the displacement maps for the IW molecules are less dense compared to the BW. The arrow lengths of the IW are found to have more heterogeneous distributions compared to the BW for all three cases. The heterogeneous nature of the map in figure 2.12 (a), (c) and (e) reveals that the IW with different mobilities are spatially correlated in both water models. The heterogeneous displacement map is indicative of dynamical heterogeneity in the system where different regions in the bilayer surface relax in different manner at any given time. Since hydrogen bonding plays a major role in confining IW in the hydrophilic region of different moieties of lipid heads, it manifests a restricted environment near lipid which differ by the chemical environment. Due to the different chemical environment, IW at different regions in the bilayer plane may follow a distribution in mobilities at a characteristic time-scale typical to their to relaxations (figure 2.12 (a), (c) and (e)) unlike the BW which are uniformly distributed over the entire bilayer surface (figure 2.12(b) and (d)).

2.9 SUMMARY

Water models in combination with lipid force-fields are not always transferable at different thermodynamic state points. Therefore, different combinations of water models and lipid force-fields do not warrant consistencies in structure and dynamics of lipids and water as in experiments. In the present study, the structure and dynamics of interface water are investigated in presence of Berger and CHARMM36 lipid bilayers in combination with TIP3P and TIP4P/2005 water models [Srivastava *et al.*, 2019b]. Since TIP3P water model is widely used for describing the dynamics of water near bio-molecules, we first test the compatibility of TIP3P water model with Berger force-field which is originally optimized for SPC water model. Previously TIP3P water model in combination with Berger force-field is found to correctly describe the thermodynamical properties of lipids in nano-discs or trans-membrane proteins in nano-discs [Debnath and Schäfer, 2015; Fisette *et al.*, 2016]. Use of TIP4P/2005 water model in combination with Berger force-field for DMPC lipids is used since bulk water dynamics is better captured by TIP4P/2005 than by TIP3P water model. The bilayer thickness, the area per head group, the order parameter, the diffusion constants and the surfce tension of the DMPC bilayer are found to be in better agreement with previously reported experimental observations using both water models in presence of Berger force-field compared to the combination with the CHARMM36 force- field. This indicates that the bilayer is at the same fluid phase as in the experiment at 308 K in presence of both water models used.

Interface water (IW) are identified if the water molecules continuously reside within a layer of ± 0.3 nm away from the average location of nitrogen lipid heads along the bilayer normal. Thus the IW molecules are associated with the choline moieties of the DMPC head groups. The oxygen-oxygen and oxygen-hydrogen RDF show that water molecules are more structured in IW compared to that in the bulk water using both models. However, correlation prevails at larger distances for oxygen-hydrogen of TIP3P IW than that of the TIP4P/2005 IW indicating more extended hydrogen bond network for TIP3P water. Hydrogen bond networks are found to play very crucial roles in determining the structure of the interface water molecules in earlier reports [Luzar and Chandler, 1996; Pasenkiewicz-Gierula *et al.*, 1997; Jana *et al.*, 2008; Re *et al.*, 2014; Srivastava and Debnath, 2018].

More back-scattering from VACF are obtained for the IW than that in the BW using both water models in presence of Berger and CHARMM36 force field. Signatures of dynamical heterogeneity are detected in all IW for all models. The initial increase in non-Gaussian parameters (NGP) for the IW reveals entrapment of the IW molecules in cages formed by the neighboring water molecules via hydrogen bonds. The values of NGP start decaying for TIP3P IW where TIP4P/2005 IW do not show a decay within the total confinement time. The decay is due to the eventual escape mechanism of water molecules from its cage to reach their diffusive limits. This indicates that the β to α relaxation has been initiated for TIP3P IW within the confinement lifetime where TIP4P/2005 IW take longer time for cage relaxations. Since TIP3P water models are known to be more diffusive, they exhibit non-Gaussian for less time than that in TIP4P/2005. No signatures of dynamical heterogeneity are found in BW associated with both models. Thus the results clearly show that TIP4P/2005 water model captures the structure and dynamics of hydration layer of a DMPC bilayer using Berger force-field at fluid phase as seen in the experiments. The present analyses i) provide a microscopic interpretation of structure of IW, ii) describe molecular motions: vibrational, local decaging, diffusive iii) demonstrate the signatures of glassy dynamics in IW, iv) examine suitability of a water model in correctly capturing structure and dynamics of hydration layers of fluid phase of the bilayer as obtained in the experiments. These analyses will be helpful in understanding dynamics of water under various conditions such as supercooling, chemical confinement and lipid phase transitions.

Several investigations regarding the study of structure and dynamics of water have been done using ab-initio molecular dynamics simulations (AIMD). Using AIMD approach, force field models are not required as the forces acting on the atoms are directly computed within the electronic structure theory. The accuracy of the data depends on the level of the exchange correlation functionals

used [Tang *et al.*, 2020]. AIMD simulations are suitable for studying structure, dynamics and SFG spectra of interfacial waters at air/water interfaces [Pezzotti *et al.*, 2018], mineral/water interfaces [Khatib *et al.*, 2016; Hosseinpour *et al.*, 2017] and so on. The results are in agreement with the IR-pump-VSFG probe experiments implying the accuracy of AIMD simulations to correctly reproduce the structure of the interfacial waters [DelloStritto *et al.*, 2018]. AIMD simulations for air/water interface systems reproduce the OH stretching, liberational and vibrational modes of interfacial water in agreement with the experimental SFG findings. Due to the accuracy in reproducing the OH spectrum of interfacial water, AIMD simulations are used over a wide range of molecular interfaces and surfaces [Liang *et al.*, 2019]. Since, AIMD simulations employ quantum chemical approach, the computational cost for carrying out the simulations is ≈ 100 times larger than typical (molecular dynamics) MD simulations using force field models. Moreover, for very large complex systems like water near a fluid lipid bilayer, the computational cost of AIMD simulations may rise upto 10^5 times than typical MD simulations [Tang *et al.*, 2020]. Therefore, the present chapter focuses on understanding the origin of slow dynamics of water near a bilayer using classical MD simulations using rigid body non-polarizable water model. These water models are successful in determining dynamics of water near soft interfaces such as proteins, bilayers [Marchi *et al.*, 2002; Kasson *et al.*, 2011; von Hansen *et al.*, 2013; Qiao *et al.*, 2019].